Vezatin is required for the maturation of the neuromuscular synapse

Natasha Koppel, Matthew B. Friese, Helene L. Cardasis, Thomas A. Neubert, and Steven J. Burden*
Helen L. and Martin S. Kimmel Center for Biology and Medicine, Skirball Institute of Biomolecular Medicine, New York University School of Medicine, New York, NY 10016

ABSTRACT Key genes, such as *Agrin*, *Lrp4*, and *MuSK*, are required for the initial formation, subsequent maturation, and long-term stabilization of mammalian neuromuscular synapses. Additional molecules are thought to function selectively during the evolution and stabilization of these synapses, but these molecular players are largely unknown. Here, we used mass spectrometry to identify vezatin, a two-pass transmembrane protein, as an acetylcholine receptor (AChR)–associated protein, and we provide evidence that vezatin binds directly to AChRs. We show that vezatin is dispensable for the formation of synapses but plays a later role in the emergence of a topologically complex and branched shape of the synapse, as well as the stabilization of AChRs. In addition, neuromuscular synapses in *vezatin* mutant mice display premature signs of deterioration, normally found only during aging. Thus, vezatin has a selective role in the structural elaboration and postnatal maturation of murine neuromuscular synapses.

INTRODUCTION

Studies of the mechanisms responsible for forming and maintaining neuromuscular synapses remain a paradigm for understanding how synapses are built and stabilized. Many of the key molecules that are required for forming neuromuscular synapses are reutilized later, as neuromuscular synapses mature and undergo structural and functional changes. There is evidence, however, suggesting that certain later adaptations, which play an important role in synaptic function and stabilization, require additional molecules, which are dispensable during synapse formation (Shi *et al.*, 2012). The molecular mechanisms that direct these later steps in the maturation of synapses, however, have received less attention than those required for the initial formation of neuromuscular synapses.

Two pathways, one transcriptional and a second posttranslational, participate to ensure that acetylcholine receptors (AChRs) are expressed at a high concentration in the postsynaptic membrane at neuromuscular synapses (Burden, 1998; Sanes and Lichtman, 2001; Wu *et al.*, 2010). The transcriptional pathway functions to boost expression of key genes, essential for synaptic function, selectively in synaptic nuclei, including those that encode the four subunits of the AChR (Burden, 1993; Schaeffer *et al.*, 2001). The posttranslational pathway acts to redistribute and anchor key postsynaptic proteins, including AChRs, in the postsynaptic muscle membrane (Burden, 1998; Sanes and Lichtman, 2001; Wu *et al.*, 2010; Tintignac *et al.*, 2015). Together, these pathways contribute to the enrichment of 20 million AChRs at each synapse, the accumulation and precise positioning of additional postsynaptic proteins, the development of postjunctional folds, as well as the formation of presynaptic specializations, including active zones, to ensure for rapid, robust, and reliable synaptic transmission (Fertuck and Salpeter, 1976; Wood and Slater, 2001).

Both pathways require four key proteins: agrin, a ligand supplied by motor neurons (McMahan, 1990; Gautam *et al.*, 1996); Lrp4, the muscle receptor for agrin (Weatherbee *et al.*, 2006; Kim *et al.*, 2008; Zhang *et al.*, 2008); MuSK, the transducing receptor tyrosine kinase (Burden *et al.*, 2013); and Dok-7 (Yamanashi *et al.*, 2012), an activator and mediator of MuSK. In contrast, rapsyn, which binds directly to AChRs, is essential for anchoring AChRs in

the postsynaptic membrane but does not act in the transcriptional pathway (Neubig *et al.*, 1979; Burden *et al.*, 1983; Gautam *et al.*, 1995; Banks *et al.*, 2003). In mice, a loss of function in any one of these genes leads to a failure to form neuromuscular synapses during development, whereas later inactivation of these genes in adult mice leads to synaptic disassembly (Tintignac *et al.*, 2015). In humans, hypomorphic mutations in any one of these genes are responsible for congenital myasthenia, a group of neuromuscular diseases that leads to muscle weakness and fatigue (Muller *et al.*, 2007; Engel *et al.*, 2015).

The AChR is a pentamer composed of four homologous subunits. Each subunit possesses four transmembrane segments and an ~100–amino acid intracellular loop, between the third and fourth transmembrane domains, that contains binding sites for rapsyn (Lee *et al.*, 2009). In addition to rapsyn, Src and adenomatous polyposis coli (APC) have been reported to bind directly to AChRs (Sobel *et al.*, 1978; Fuhrer and Hall, 1996; Wang *et al.*, 2003). The role of APC at neuromuscular synapses has not been studied, but Src-family kinases represent one set of molecules that are required for stabilizing but not forming neuromuscular synapses (Smith *et al.*, 2001). To identify additional AChR-associated proteins that might play a role in the development of neuromuscular synapses, we isolated AChRs from muscle and used mass spectrometry (MS) to identify proteins that coisolate with AChRs. Here, we show that vezatin, a transmembrane protein that is enriched at adherens junctions in epithelial cells, binds to AChRs, is concentrated in the postsynaptic membrane at neuromuscular synapses, and has an important role in the postnatal maturation and maintenance of neuromuscular synapses.

RESULTS

Vezatin is an AChR-associated protein

To identify AChR-associated proteins, we isolated AChRs from cultured myotubes and analyzed the protein composition of the AChR complex by MS. Because we also sought to determine whether agrin stimulation might lead to a change in the composition of the AChR protein complex, we used stable isotope labeling with amino acids in cell culture (SILAC) to separately label proteins in myotubes treated with or without neural agrin (Figure 1A). One set of myotube cultures was grown in media with normal amino acids and treated with agrin, whereas the other set of myotube cultures was grown in media with heavy amino acids. Lysates from the two sets of cultures were pooled, AChRs were isolated with biotin-conjugated α-bungarotoxin (α-BGT), and the composition of proteins in the complex was analyzed by liquid chromatography (LC)–MS (see *Materials and Methods*).

We focused our attention on AChR-associated proteins that were identified by recovery of three or more peptides and showed a ≥1.25-fold increase in association with AChRs upon agrin stimulation. This analysis identified six proteins, including rapsyn (Figure 1, A and B; Supplemental Table S1). Their increased association with AChRs following agrin treatment was modest, ~1.3-fold (Figure 1B; Supplemental Table S1). Notably, we did not detect proteins that altered their association with AChRs by more than 1.35-fold, inconsistent with the idea that one or more proteins associate with AChRs only after agrin stimulation. Two of the AChR-associated proteins, rapsyn and CAMKII, are known synaptic proteins (Sobel *et al.*, 1978; Neubig *et al.*, 1979; Froehner *et al.*, 1981; Martinez-Pena y Valenzuela *et al.*, 2010), and ubiquitin is attached to AChRs and enriched at neuromuscular synapses (Serdaroglu *et al.*, 1992). Western blotting confirmed the association of annexin A2 but not enolase with AChRs. Moreover, our MS experiments did not detect all proteins that are present in a complex with AChRs, as we found α-actinin but

not other rapsyn-associated proteins, including calpain, β-catenin, and Macf1 (Antolik *et al.*, 2007; Chen *et al.*, 2007; Zhang *et al.*, 2007; Dobbins *et al.*, 2008; Figure 1C; Supplemental Table S1).

Vezatin binding to AChRs does not require rapsyn

Among these six proteins found to coisolate with AChRs, we chose to study vezatin further, in part because vezatin, an ~125 kDa, two-pass transmembrane protein, is expressed and plays a role at other cell–cell junctions, including adherens junctions (Kussel-Andermann *et al.*, 2000; Hyenne *et al.*, 2005; Bahloul *et al.*, 2009). To confirm the findings from the MS studies, we probed Western blots of the AChR complex, isolated with biotin-conjugated α-bungarotoxin (BGT) from C2C12 myotubes, with two different antibodies to vezatin. Figure 1 shows that vezatin coisolated with AChRs, confirming the findings from the MS analysis (Figure 1B). Moreover, Western blotting showed an agrin-dependent increase (1.6-fold) in association of vezatin with AChRs, similar to the results from the SILAC/MS experiments (Figure 1B).

We next sought to determine whether vezatin binds directly or indirectly to AChRs. Three proteins, rapsyn, Src, and APC bind directly to AChRs, whereas other AChR-associated proteins require rapsyn for their coisolation with AChRs (Sobel *et al.*, 1978; Fuhrer and Hall, 1996; Wang *et al.*, 2003; Oury *et al.*, 2019). We isolated AChRs from muscle of *rapsn*^{+/–} control and *rapsn*^{–/–} mutant mice and measured the amount of vezatin that coisolated with AChRs by Western blotting. Figure 1 shows that vezatin, unlike α-actinin, coisolated with AChRs independent of rapsyn, indicating that rapsyn does not mediate the association between vezatin and AChRs (Figure 1C). Indeed, 1.8-fold more vezatin associated with AChRs in the absence of rapsyn (Figure 1C), suggesting a partial competition between rapsyn and vezatin for binding to AChRs (see below).

To determine whether vezatin binds to AChRs, we coexpressed epitope-tagged vezatin and fusion proteins, containing the main intracellular region (MA) of individual AChR subunits that were linked to the extracellular and transmembrane regions from CD4 (Lee *et al.*, 2009). We immunoprecipitated CD4-AChR subunit MA loop chimeras from the cotransfected HEK 293 cells with antibodies to CD4, and Western blots were probed with antibodies to Flag or CD4. Figure 2 shows that 30-fold more vezatin associated with the CD4-AChR β subunit fusion protein than CD4 alone. Vezatin associated less well with AChR δ and ε subunit fusion proteins (Figure 2). Although we cannot exclude the possibility that binding between vezatin and AChR subunits requires other proteins expressed in HEK 293 cells, these data are consistent with the idea that vezatin binds directly to AChRs and that binding can be mediated by multiple AChR subunits.

Because rapsyn also binds the AChR β subunit, we wondered whether rapsyn and vezatin bind to overlapping regions within the MA of the AChR β subunit. We coexpressed Flag-tagged vezatin, CD4-AChR β, and HA-tagged rapsyn to learn whether rapsyn expression impaired association between vezatin and CD4-AChR β. Supplemental Figure S1 shows that rapsyn expression reduced association between vezatin and CD4-AChR β by fourfold, indicating that vezatin and rapsyn compete, at least in part, for binding to the AChR β subunit. These findings are consistent with the increased association between vezatin and AChRs in *rapsn* mutant myotubes (Figure 1C) and suggest that vezatin and rapsyn bind to overlapping sequences in the AChR β subunit.

The MA from the AChR δ subunit binds vezatin but not rapsyn (Figure 2; Lee *et al.*, 2009). Consistent with these findings, HA-rapsyn expression failed to diminish binding between vezatin and
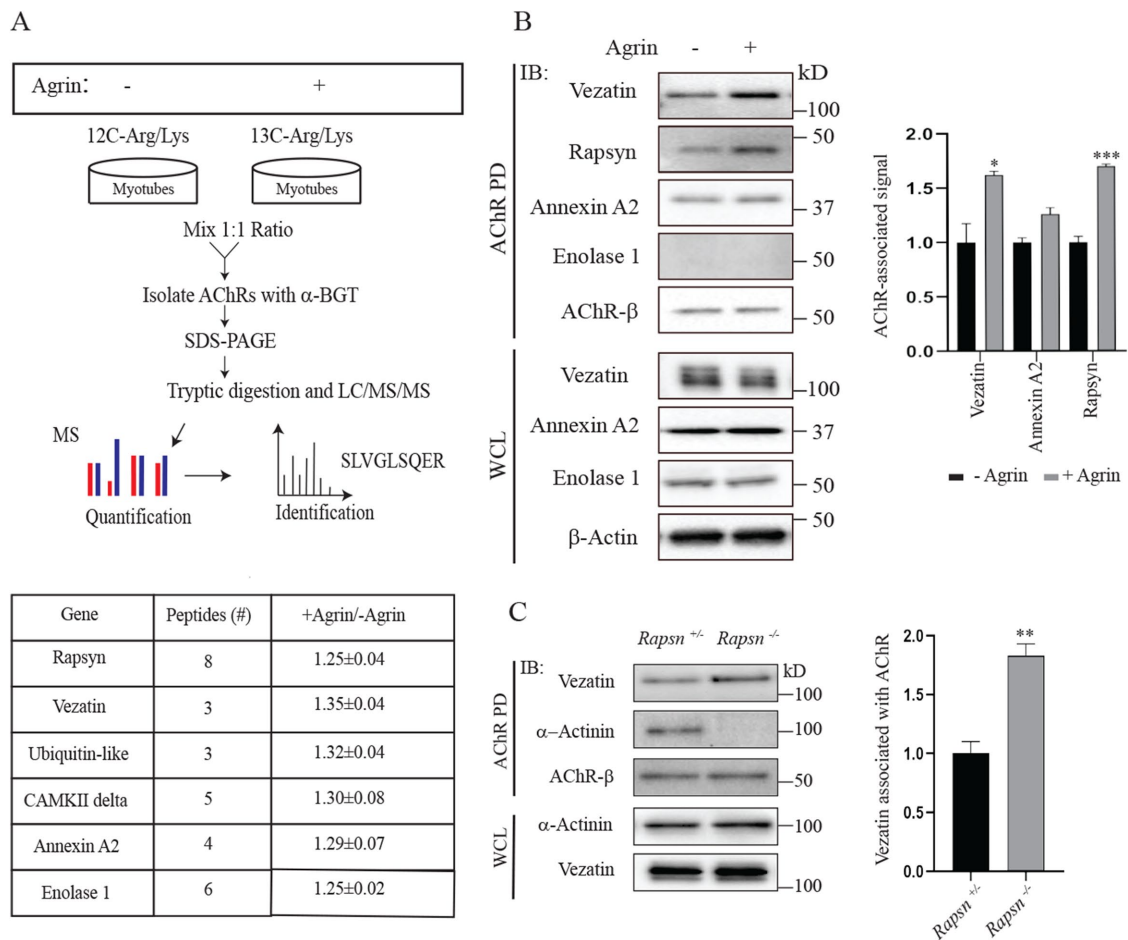
FIGURE 1: Vezatin associates with AChR in a rapsyn-independent manner. (A) Myotubes were grown in media containing heavy isotopes of lysine and arginine or in normal media. Myotubes labeled in normal media were stimulated with agrin while myotubes grown in media with heavy amino acids were not treated with agrin. Lysates from agrin-treated and nontreated myotubes were mixed in a 1:1 ratio, and AChRs, together with AChR-associated proteins, were isolated with biotin-conjugated α-BGT. Isolated proteins were resolved by SDS–PAGE and identified by mass spectrometry. Proteins that associated preferentially with AChRs in agrin-treated myotubes are indicated. (B) Western blots of the AChR complex isolated from agrin-treated C2C12 myotubes were probed with antibodies to vezatin, rapsyn, annexin A2, enolase 1, or the AChR β subunit ($n = 3$). The Western blotting experiments confirmed the association of rapsyn, vezatin, and annexin A2 but not enolase 1 with AChRs. (C) AChRs and AChR-associated proteins were isolated from muscle lysates of E17.5 *rapsn*^{+/–} control and *rapsn*^{–/–} mice with biotin-conjugated α-BGT ($n = 3$). Rapsyn is required for the association of α-actinin but not vezatin with AChRs. The association of vezatin with AChRs increased by 1.8-fold in the absence of rapsyn ($n = 4$ for *rapsn*^{+/–} and $n = 3$ for *rapsn*^{–/–}). Error bars indicate SEM, and p values were calculated using an unpaired t test (*, $p < 0.05$; **, $p < 0.005$; ***, $p < 0.0005$).

CD4-AChR δ (Supplemental Figure S1). These data indicate that rapsyn and vezatin have the potential to bind simultaneously to AChRs by binding separately to the β and δ subunits.

Agrin stimulates tyrosine phosphorylation of the the AChR β subunit, which is responsible for the increased association between AChRs amd rapsyn following agrin treatment (Borges *et al.*, 2008; Lee *et al.*, 2009). The similar increase in association between vezatin and AChRs following agrin stimulation suggested that this additional recruitment may also be due to tyrosine phosphorylation of the AChR β subunit. We therefore treated C2 myotubes with agrin in the presence or absence of staurosporine or herbimycin, tyrosine kinase inhibitors that inhibit phosphorylation of the AChR β subunit. We isolated the AChR complex and probed Western blots with antibodies to vezatin, phosphotyrosine, or the AChR β subunit. Supplemental Figure S2 shows that the agrin-stimulated increase in association between vezatin and AChRs is prevented by inhibiting

tyrosine kinases and AChR β subunit phosphorylation (Supplemental Figure S2). Thus, like rapsyn, vezatin appears to associate both constitutively and in a phosphorylation-dependent manner with AChRs.

Vezatin is concentrated at the postsynaptic membrane at neuromuscular synapses

We stained frozen sections of skeletal muscle with antibodies to vezatin to determine whether vezatin is enriched at neuromuscular synapses. Figure 3 shows that vezatin is enriched at neuromuscular synapses (Figure 3A). To determine whether vezatin is expressed in the postsynaptic membrane, we stained single, dissected myofibers, lacking presynaptic nerve terminals, with α-BGT and antibodies to vezatin. Figure 3 shows that vezatin is enriched at synaptic sites, marked by AChRs but lacking nerve terminals (Figure 3B). These findings indicate that vezatin is a postsynaptic protein,
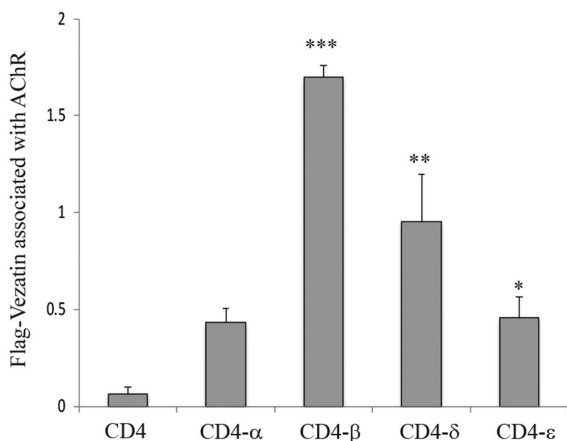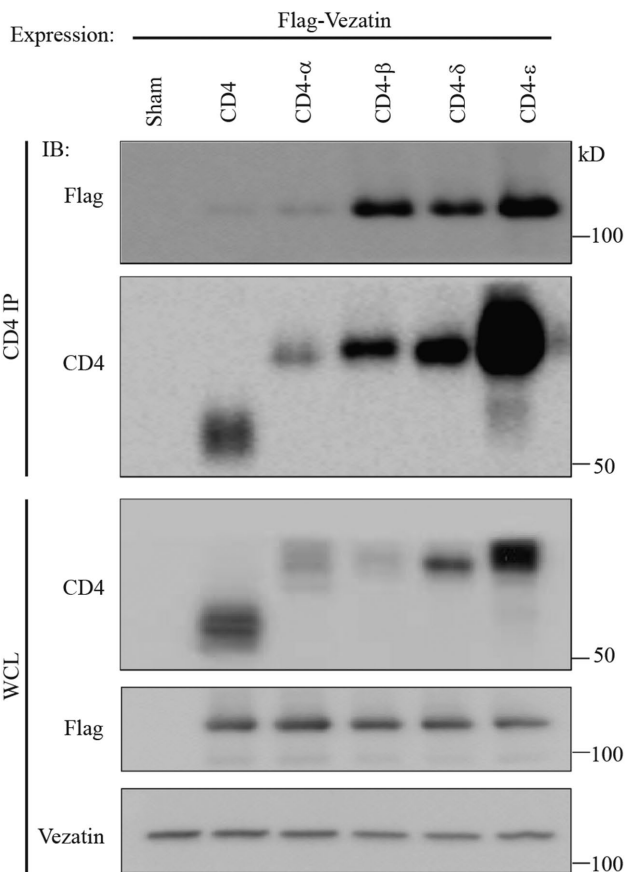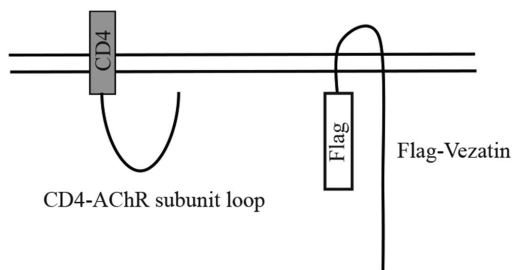
FIGURE 2: Vezatin associates with AChR subunits. cDNAs encoding Flag-vezatin and CD4-AChR subunit MA loop chimeras were cotransfected into HEK 293 cells. CD4-AChR subunit MA loop chimeras were immunoprecipitated with antibodies to CD4, and Western blots were probed with antibodies to Flag or CD4. The four CD4-AChR subunit chimeras were expressed at different levels, so the

consistent with the experiments showing that vezatin associates with the intracellular region of AChRs (Figure 1).

Vezatin is not essential for synapse formation

To determine whether vezatin has a role in neuromuscular synapse formation, we inactivated *vezt* selectively in skeletal muscle. We crossed mice carrying floxed and null alleles of *vezt* (Hyenne *et al.*, 2007) with mice carrying a *human skeletal actin (hsa)::cre* transgene (Miniou *et al.*, 1999), which is expressed in myotubes but not in myoblasts. We quantified the loss of vezatin in muscle by isolating AChRs from lysates of embryonic limb muscle and measuring the amount of vezatin that coisolated with AChRs. We found that vezatin levels were reduced by nearly 10-fold (Figure 4A). *Vezt^{F/−}; hsa::cre* mice were recovered postnatally at the expected Mendelian frequency and adult mutant mice were fertile, indicating that the formation and function of muscle and neuromuscular synapses were impaired little, if at all. Consistent with these findings, histological analysis of *vezt^{F/−}; hsa::cre* mice revealed a normal number of myofibers both shortly after birth and in adult mice (Figure 4, B and C, and Supplemental Figure S3). Moreover, the cross-sectional area and ultrastructure of muscle fibers, including the organization of sarcomeres, appeared normal in *vezt^{F/−}; hsa::cre* mice (Figure 4, B and C, and Supplemental Figure S3).

During development, motor axons branch and terminate in a band of synapses that are adjacent to the main intramuscular nerve in the middle of the muscle. Each muscle fiber is innervated at a single synaptic site, which is marked by the accumulation of synaptic vesicles in nerve terminals and a high concentration of AChRs in the postsynaptic membrane (Sanes and Lichtman, 2001). To determine whether vezatin has a role in organizing presynaptic and postsynaptic differentiation, we stained whole mounts of the diaphragm muscle from E17.5 mice with probes that mark motor axons, nerve terminals, or AChRs (Figure 4E). AChRs in muscle from *vezt^{F/−}; hsa::cre* mice were concentrated in ovoid plaques, which were opposed by nerve terminals (Figure 4E), indistinguishable from the organization of AChRs and synapses at developing neuromuscular synapses in *vezt^{F/+}* control mice. Although synapses in *vezt^{F/−}; hsa::cre* mice were distributed in a modestly wider band within the central region of the muscle (Figure 4G), the number and size of synapses and the density of synaptic AChRs were normal (Figure 4F). Thus, major features of synapse formation occurred normally in mice deficient in vezatin muscle expression.

Vezatin plays a role in synapse maturation

The formation, maturation, and maintenance of neuromuscular synapses require core components, such as agrin, Lrp4, MuSK, and Dok-7 at each stage. Certain genes, however, such as those encoding Src-family kinases, dystroglycan, and α-dystrobrevin, are required for the maturation but not the formation of synapses (Grady *et al.*, 1997, 2000, 2003; Smith *et al.*, 2001; Shi *et al.*, 2012). Therefore, we determined whether vezatin might be required for these later steps in synapse development.

During the first 3 wk after birth, neuromuscular synapses undergo multiple maturation steps: ovoid AChR plaques evolve to form

amount of coprecipitated Flag-vezatin was normalized to the expression level of each CD4-AChR subunit MA loop chimera (*n* = 3). Thirty-fold more Flag-vezatin associated with the CD4-β chimeras than CD4 alone (*n* = 3). Vezatin also associated with the AChR δ, AChR ε, and AChR α subunit chimeras. Error bars indicate SEM, and *p* values were calculated using an unpaired *t* test (*, *p* < 0.05; **, *p* < 0.005; ***, *p* < 0.0005).
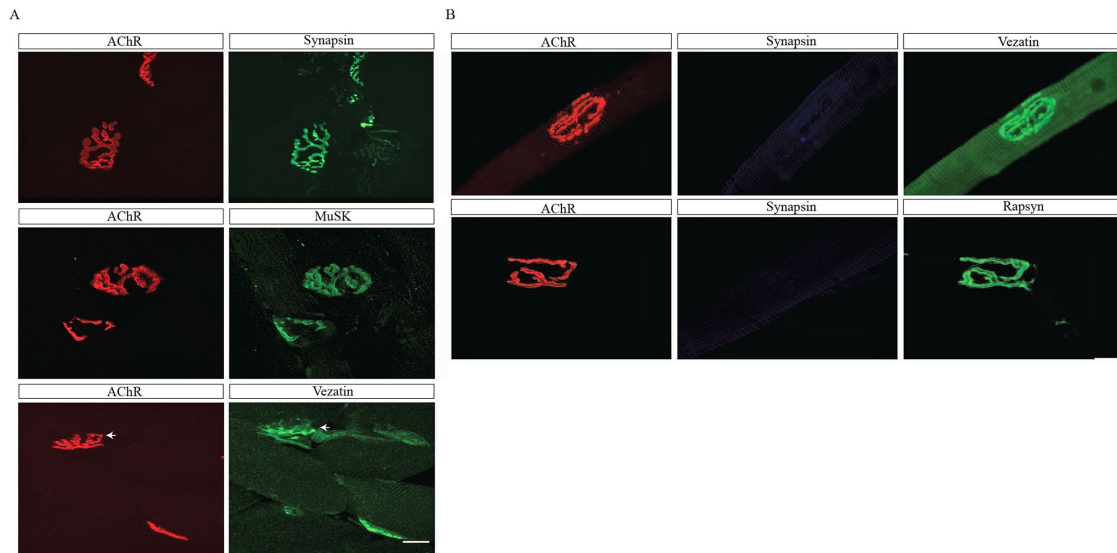
FIGURE 3: Vezatin is enriched at the postsynaptic membrane at neuromuscular synapses. (A) Cross-sections of innervated adult mouse gastrocnemius muscles were stained with Alexa 594–conjugated α-BGT to label AChRs, antibodies to synapsin to label nerve terminals, and antibodies to vezatin or MuSK. Vezatin is enriched at synaptic sites (arrows). (B) Single muscle fibers from adult TA muscles were dissociated and stained with Alexa 594–conjugated α-BGT, antibodies to synapsin, and antibodies to vezatin or rapsyn. Most dissociated myofibers lacked nerve terminals. Vezatin remained enriched at synaptic sites in the absence of nerve terminals. Scale bar = 20 μm.

convoluted, branched, and pretzel-like shapes, synapses are eliminated, the AChR γ subunit is replaced by the ε subunit, the turnover rate of AChRs becomes prolonged, and the postsynaptic membrane develops deep and regular invaginations, termed postjunctional folds (Hall and Sanes, 1993).

This transition from an ovoid to a pretzel-like shape occurs in stages, as ovoid AChR plaques first develop perforations and then become c-shaped (Figure 5, A and D). These three immature arrangements of synaptic AChRs largely disappear by 1 mo after birth, when branched, pretzel-like shapes predominate (Kummer *et al.*, 2004). Development of the mature shape is impaired in $vezt^{F/-}$; *hsa::cre* mice (Figure 5, A and E). First, in control $vezt^{F/+}$ mice at P60, only 6.5% of synapses appear immature, whereas ~50% of synapses in $vezt^{F/-}$; *hsa::cre* mice remain immature at P60 (48.6 ± 6.7%, $n = 232$ for $vezt^{F/-}$; *hsa::cre* mice; 6.5 ± 1.6%, $n = 286$ for $vezt^{F/+}$ mice; Figure 5E). Second, whereas synaptic AChRs are arranged in a nearly continuous manner, interrupted by few breaks in control P60 $vezt^{F/+}$ mice (0 ± 0%, $n = 286$), this arrangement was perturbed in $vezt^{F/-}$; *hsa::cre* mice, as synaptic fragmentation was more common and extensive (5.3% ± 0.7, $n = 232$; Figure 5E). Third, although the size of synapses in $vezt^{F/-}$; *hsa::cre* mice was normal (Figure 5B), the density of synaptic AChRs was reduced by 20% (100 ± 1.8%, $n = 286$ for $vezt^{F/+}$ mice; 80.7 ± 4.3%, $n = 232$ for $vezt^{F/-}$; *hsa::cre* mice; Figure 5C). Because $vezt^{F/-}$; *hsa::cre* mice failed to show signs of motor impairment (Suppemental Figure S3), the retention of simply shaped synapses and the 20% decrease in density of synaptic AChRs, which is insufficient on its own to impair synaptic transmission (Wood and Slater, 2001), led to no apparent detriment in motor function.

The development of postjunctional folds is defective in *vezt* mutant mice

To determine whether postjunctional folds developed normally in the absence of vezatin, we analyzed the structure of neuromuscular synapses in P30 $vezt^{F/+}$ control and $vezt^{F/-}$; *hsa::cre* mice by electron microscopy (Figure 5F). The overall organization of synapses in

$vezt^{F/-}$; *hsa::cre* mice appeared normal, as nerve terminals, capped by terminal Schwann cells and containing synaptic vesicles, were juxtaposed to the postsynaptic membrane and separated from the postsynaptic membrane by the synaptic basal lamina. Postjunctional folds were present at *vezt* mutant synapses, but the extent of folding was reduced by 15% (2.5 ± 0.2, $n = 48$ for $vezt^{F/+}$ mice and 2.1 ± 0.1, $n = 81$ for $vezt^{F/-}$; *hsa::cre* mice; Figure 5G), and the number of postjunctional folds with mouths that opened into the synaptic cleft was reduced by 31% (1.1 ± 0.1 mouths/μm, $n = 48$ for $vezt^{F/+}$ mice and 0.8 ± 0.1 mouths/μm, $n = 81$ for $vezt^{F/-}$; *hsa::cre* mice; Figure 5G). Taken together, these defects in the organization of postjunctional folds may contribute to the decreased density of synaptic AChRs.

The stability of AChR clusters is reduced in myotubes lacking vezatin

AChR clusters disassemble if they are not stabilized by agrin/MuSK signaling (Grady *et al.*, 2000; Lin *et al.*, 2001; Smith *et al.*, 2001; Yang *et al.*, 2001; Kim *et al.*, 2008). Because vezatin has a role in synaptic maturation, we wondered whether vezatin might have a role in stabilizing AChR clusters. We treated cultures of primary myotubes, derived from control or $vezt^{F/-}$; *hsa::cre* mice, overnight with agrin and then withdrew agrin to measure the stability of AChR clusters. Myotubes from $vezt^{F/+}$ and $vezt^{F/-}$; *hsa::cre* mice differentiated and responded similarly to agrin treatment (Figure 6, A and B). Following Agrin withdrawal, however, AChR clusters in control myotubes disassembled with a half-life of 12 h, whereas AChRs clusters in *vezt*-deficient myotubes dispersed with a half-life of 5 h (Figure 6, B and C). These results indicate that vezatin, like Src-family kinases and α-dystrobrevin, plays a role in stabilizing AChR clusters.

The structure of the neuromuscular synapse deteriorates in *vezt* muscle-conditional mutant mice

Neuromuscular synapses deteriorate during aging, evident by an increased frequency in preterminal axon swellings, dystrophic axons, and fragmentation in the organization of AChRs. These
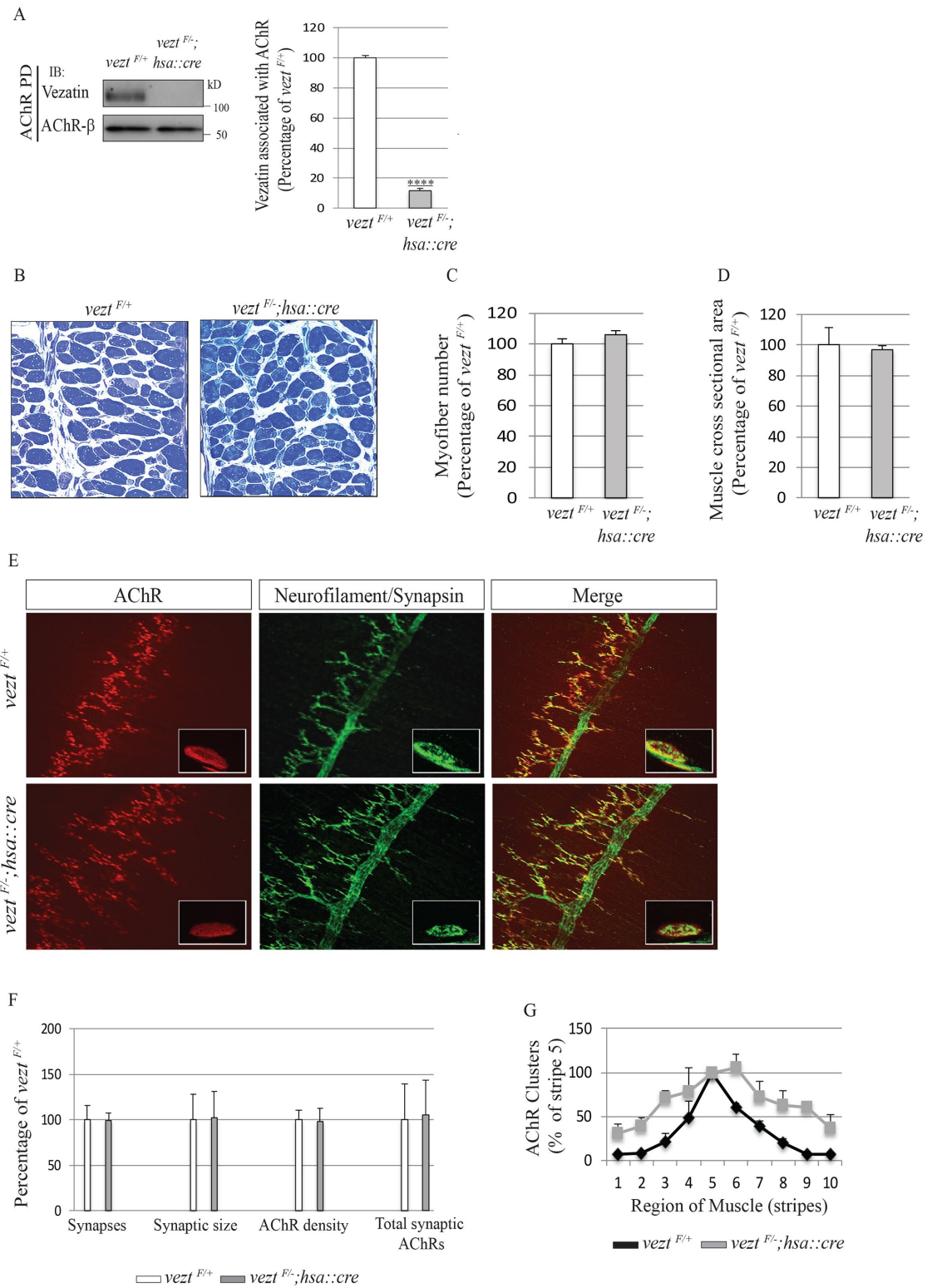
FIGURE 4: Vezatin is dispensable for neuromuscular synapse formation. (A) AChRs were isolated from muscle lysates of *vezt^F/+* control and *vezt^F/−; hsa::cre* mice with biotin-conjugated α-BGT, and Western blots were probed with antibodies to vezatin or the AChR β subunit. AChR-associated vezatin levels were reduced nearly 10-fold in *vezt^F/−; hsa::cre* mice. (B–D) Toluidine blue–stained cross-sections of diaphragm muscles showed a normal number and size of myofibers in E17.5 *vezt^F/−; hsa::cre* mice with normal cross-sectional area. Scale bar = 50 μm. (E) Whole mounts of diaphragm muscles from E17.5 *vezt^F/+* and *vezt^F/−; hsa::cre* mice were stained with Alexa 594–conjugated α-BGT, and antibodies to neurofilament and synapsin to visualize AChRs (red) and axons and nerve terminals (green). Scale bar = 250 μm. (F) The number of synapses, synaptic area, synaptic AChR density, and total synaptic AChRs were normal in the absence of vezatin. (G) The distribution of synapses was modestly wider in the absence of vezatin. Error bars indicate SEM, *n* = 3 mice, and *p* values were calculated using an unpaired *t* test (****, *p* < 0.00005).
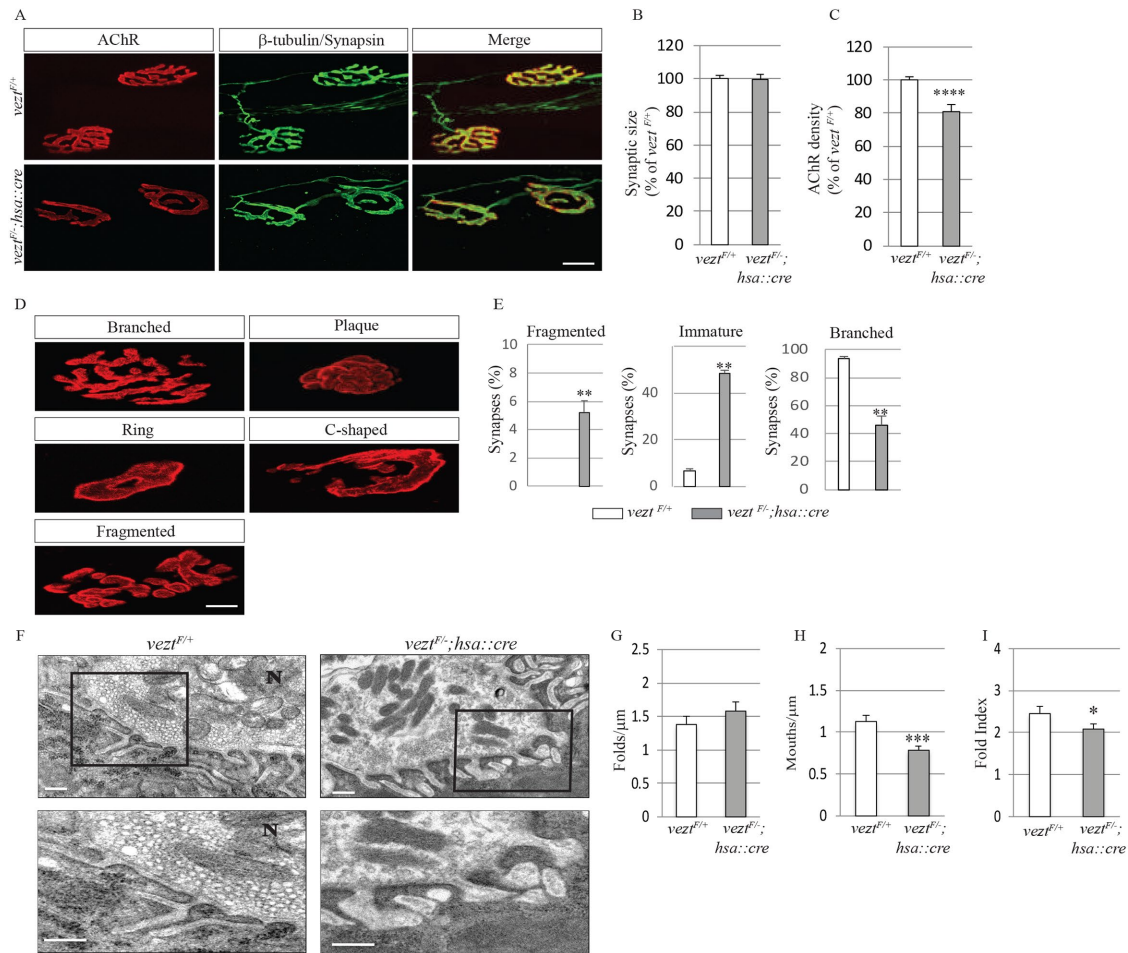
FIGURE 5: Vezatin is required for the maturation of neuromuscular synapses. (A) Diaphragm muscles from P60 *vezt*$^{F/+}$ and *vezt*$^{F/-}$; *hsa::cre* mice were stained with Alexa 594–conjugated α-BGT, β-tubulin, and synapsin to visualize AChRs (red) as well as axons and nerve terminals (green). Scale bar = 10 μm. (B, C) In the absence of vezatin, synaptic size was normal but the density of synaptic AChRs was reduced. (D, E) In the absence of vezatin, most neuromuscular synapses remained immature and more synapses were fragmented, whereas synapses in control mice were largely branched and complex. Mature synapses were defined as containing three to five gaps in AChR-rich areas while immature synapses were defined as containing ≤2 gaps in AChR-rich areas. Fragmented synapses were defined as containing >5 gaps in AChR-rich areas (Latvanlehto *et al.*, 2010). Error bars indicate SEM. Values were obtained from *n* = 3 mice (286 synapses for *vezt*$^{F/+}$ and 232 synapses for *vezt*$^{F/-}$; *hsa::cre*). Scale bar = 20 μm. (F) In the absence of vezatin, nerve terminals (N), containing normal numbers of synaptic vesicles and mitochondria, are apposed to the postsynaptic membrane with postjunctional folds. The postsynaptic membranes in both *vezt*$^{F/+}$ and *vezt*$^{F/-}$; *hsa::cre* mice are electron dense at the crests and upper portions of the postjunctional folds. Scale bar = 500 nm. (G–I) The number of postjunctional folds (folds/μm) was normal, while the fold index and fold mouths/μm were reduced in *vezt*$^{F/-}$; *hsa::cre* mice. Fold index was calculated by dividing the length of the total postjunctional fold membrane by the length of the synaptic cleft. Fold mouths were defined as openings to the synaptic cleft (Friese *et al.*, 2007). Error bars indicate SD. Values were obtained from *n* = 3 mice (48 synapses for *vezt*$^{F/+}$ and 81 synapses for *vezt*$^{F/-}$; *hsa::cre*). *p* values were calculated using an unpaired *t* test (*, $p < 0.05$; **, $p < 0.005$; ***, $p < 0.0005$; ****, $p < 0.00005$).

alterations are normally evident at 18 mo of age and more common and severe by 2 yr of age in mice (Valdez *et al.*, 2010). Because we observed fragmented synapses, a hallmark of aging synapses, in P60 *vezt*$^{F/-}$; *hsa::cre* mice (Figure 5E), we wondered whether *vezt* mutant synapses might show other premature signs of deterioration. We analyzed synapses in diaphragm muscles from *vezt*$^{F/+}$ control and *vezt*$^{F/-}$; *hsa::cre* P180 mice (Figure 7). Although we found no evidence for an increase in axonal sprouting or denervation, swollen preterminal motor axons were fivefold more common in *vezt* conditional mutant mice than control mice (37.2 ± 4.2% vs. 7 ± 1.0%; Figure 7, A and B). Moreover, dystrophic axons (5.7 ± 0.3 vs. 17 ± 1.2) and postsynaptic fragmentation (16.4 ± 0.2 vs. 37.2 ± 4.2) were

two- to threefold more common in *vezt* muscle-conditional mutant mice (Figure 7, A and B). Thus, the loss of vezatin from muscle leads not only to defects in maturation of the postsynaptic membrane but also to signs of motor axon deterioration, normally evident in aging mice.

DISCUSSION
Here, we show that vezatin binds to AChRs and regulates the maturation of neuromuscular synapses and stabilization of AChRs. In the absence of vezatin, neuromuscular synapses fail to undergo the normal plaque to pretzel shape transition that is a characteristic and hallmark feature of rodent neuromuscular synapses. Thus,
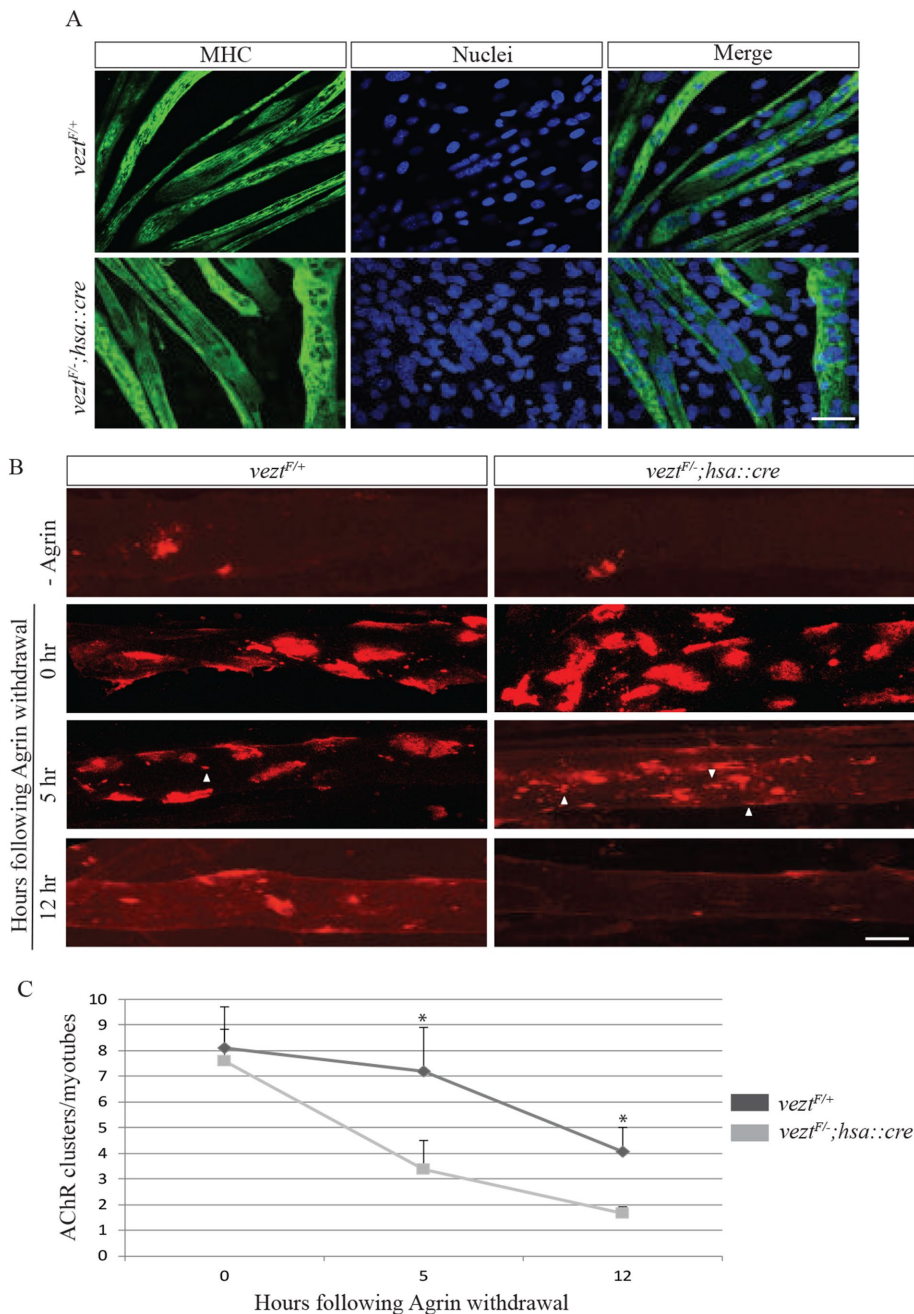
FIGURE 6: Vezatin stabilizes agrin-induced AChR clusters. (A) $vezt^{F/+}$ and $vezt^{F/-}$; $hsa::cre$ mutant myotubes, stained for myosin heavy chain (MHC), differentiated similarly. Scale bar = 50 µm. (B, C) Myotubes were treated overnight with agrin to induce AChR clusters and subsequently cultured in the absence of agrin for 5 h or 12 h. In $vezt^{F/+}$ myotubes, agrin-induced AChR clusters had a half-life of 12 h, whereas the half-life of agrin-induced AChR clusters in $vezt$ mutant myotubes was 5 h. Arrowheads indicate AChR microclusters (2–5 µm in diameter). Error bars indicate SEM ($n = 3$ at each time point), and p values were calculated using an unpaired t test (*, $p < 0.05$). Scale bar = 20 µm.

the neuromuscular synapse is compact, like in mammals, but the contact is simple and lacks a pretzel-like shape and prominent postjunctional folds (Burden, 1977). In humans, neuromuscular synapses are unusually small with particularly extensive and deep postjunctional folds (Couteaux, 1955; Slater, 2017). As such, although agrin, Lrp4, MuSK, and rapsyn play key roles in the formation of neuromuscular synapses in all vertebrates (Tintignac et al., 2015), there appears to be a wide latitude in the particular shape that a neuromuscular synapse can adopt, possibly explaining the lack of a motor deficit in $vezt$ muscle-conditional mutant mice, in which synapses fail to fully transition from an immature to a pretzel-like shape. Nonetheless, because the extensive and deep folding of the postsynaptic membrane at human neuromuscular synapses plays an important role in synaptic transmission at these small synapses, it remains possible that the aberrant organization of postjunctional folds, found in $vezt$ conditionally mutant mice, would have a more profound effect on synaptic function in humans harboring mutations in $vezt$.

Vezatin, like rapsyn, associates with AChRs. Rapsyn, a 43 kDa intracellular, peripheral membrane protein, binds to AChRs and plays a critical role in the anchoring of AChRs at neuromuscular synapses (Burden et al., 2018). In nonmuscle cells that express the MA from individual AChR subunits, fused to CD4, rapsyn binds to the β, α, and ε subunits but not to the AChR δ subunit (Lee et al., 2009). Using the same experimental paradigm, vezatin binds to the AChR β subunit and less well to the AChR δ and ε subunits. Because vezatin, unlike rapsyn, can bind the AChR δ subunit, the AChR possesses both shared and unique binding sites for vezatin and rapsyn. Although these findings do not reveal how vezatin or rapsyn binds to fully assembled AChR pentamers, these experiments, together with competition experiments, indicate that vezatin and rapsyn bind to overlapping regions within the MA of the AChR β subunit. As such, changes in the level of vezatin expression have the potential to modify association of rapsyn with the AChR β subunit, and vice versa.

Despite the overlap in binding to the AChR β subunit, rapsyn and vezatin do not function in a redundant manner: AChRs do not cluster and neuromuscular synapses fail to form in the absence of rapsyn (Gautam et al., 1995), whereas vezatin has a role in the maturation and stabilization of neuromuscular synapses (Grady et al., 1997, 2000, 2003; Smith et al., 2001; Shi et al., 2012). How rapsyn anchors AChRs and other postsynaptic proteins at the postsynaptic membrane is poorly understood (Li et al., 2016; Burden et al., 2018). Structural studies demonstrate that purified, membrane-bound AChRs can be found

vezatin joins Src-family kinases, utrophin, and α-dystrobrevin as synaptic proteins that have roles in the postnatal maturation but not the formation of murine neuromuscular synapses.

The shape of the neuromuscular synapse is not conserved but widely divergent among different vertebrate classes (Couteaux, 1955; Slater, 2017). For example, although the synapse is compact in mammals, the neuromuscular synapse in amphibians extends in multiple, long stripes, each several hundred micrometers in length. In avians,
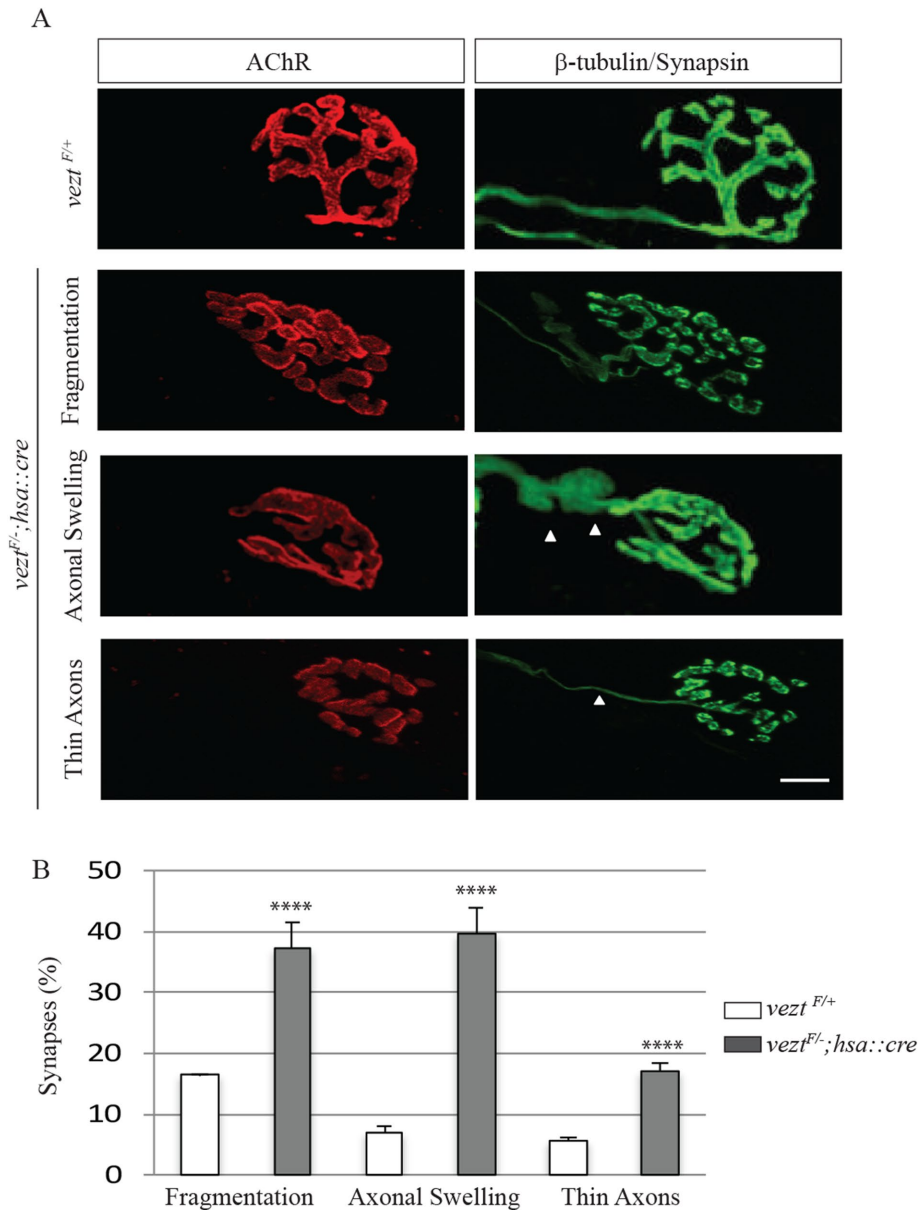
FIGURE 7: Vezatin is required to maintain synapses in adult mice. (A) Diaphragm muscles from P180 *vezt*$^{F/+}$ and *vezt*$^{F/-}$; *hsa::cre* mice were stained with Alexa 594–conjugated α-BGT, β-tubulin, and synapsin to visualize AChRs (red) and axons and nerve terminals (green). Three characteristics of synaptic deterioration were apparent in *vezt*$^{F/-}$; *hsa::cre* mice. (B) In *vezt*$^{F/-}$; *hsa::cre* mice, the frequency of synaptic fragmentation, axonal dystrophy, and thin axons were increased. Arrowheads indicate either axonal swellings or thin axons. Scale bar = 20 μm. Error bars indicate SEM. Values were obtained from n = 3 mice (n = 140 synapses for *vezt*$^{F/+}$ and n = 165 synapses for *vezt*$^{F/-}$; *hsa::cre*), and p values were calculated using an unpaired t test (****, $p < 0.00005$).

recruitment of vezatin to tyrosine phosphorylated AChRs contributes to the stabilization of AChRs and maturation of neuromuscular synapses during postnatal development.

Because the *hsa::cre* gene is activated as myotubes begin to form at ~E10 (Miniou *et al.*, 1999), whereas neuromuscular synapses form on multinucleated myotubes at ~E13 (Sanes and Lichtman, 2001), our findings indicate that vezatin is not essential for neuromuscular synapse formation. However, vezatin expression in neonatal muscle was not eliminated but reduced by 10-fold in *vezt*$^{F/-}$; *hsa::cre* mice. Residual vezatin, present at E18.5, may be a result of incomplete *vezt* gene inactivation in myotubes or persistent vezatin protein that was synthesized earlier in myoblasts, or both. In either case, it remains possible that the residual vezatin is sufficient to initiate early events in synapse formation. Similarly, it remains possible that vezatin has a more important role in synaptic maintenance than revealed here, as the low level of vezatin in adult muscle of *vezt*$^{F/-}$; *hsa::cre* mice may be adequate to promote aspects of synapse maturation.

A major form of vezatin contains two intracellular regions, separated by two transmembrane segments and a short extracellular region (Bahloul *et al.*, 2009). Because binding between vezatin and the AChR is mediated by the MA in the AChR β and δ subunits, one or both of the intracellular regions from vezatin are likely to bind directly to the AChR. The intracellular region of vezatin binds myosin VIIa and radixin, through their FERM domains, and to Arf6 (Kussel-Andermann *et al.*, 2000; Bahloul *et al.*, 2009; Sanda *et al.*, 2010). In addition, in epithelial cells, vezatin coimmunoprecipitates together with cadherin and α-catenin, likely mediated by an indirect association between vezatin and α-catenin (Kussel-Andermann *et al.*, 2000; Sousa *et al.*, 2004). Although cadherins are expressed by presynaptic Schwann cells, there is little, if any, evidence that cadherins are present in the postsynaptic muscle cell membrane (Cifuentes-Diaz *et al.*, 1994, 1996, 1998). Although myosin VIIa and radixin have similarly not been reported to function at neuromuscular synapses, Arf6 has a role in regulating endosomal trafficking of MuSK (Luiskandl *et al.*, 2013). As such, it is possible that recruitment of Arf6 to AChR-bound vezatin may have a role in regulating MuSK trafficking and synaptic maturation. Alternatively, the recruitment of Arf6 could play a role in shaping the postsynaptic membrane and organizing postjunctional folds, as Arf6 has roles in membrane trafficking and shaping other membranes (Donaldson, 2003; Donaldson *et al.*, 2009). Further studies will be required to better understand the mechanisms by which vezatin, as well as Src-family kinases, utrophin, and α-dystrobrevin regulate synaptic maturation.

with one, two or three molecules of rapsyn attached (Zuber and Unwin, 2013). These findings suggest that binding of a third molecule of rapsyn to AChRs, likely to the tyrosine phosphorylated AChR β subunit, creates an extensive 2D lattice that may be important for stabilizing AChR clusters (Zuber and Unwin, 2013). Consistent with this idea, in the absence of AChR β subunit tyrosine phosphorylation, mutant AChRs can cluster at synapses and in cultured myotubes treated with agrin, but these AChR clusters are unstable, as they disassemble following agrin withdrawal, and the mutant, non-phosphorylated AChRs are rapidly solubilized by nonionic detergent (Friese *et al.*, 2007; Borges *et al.*, 2008). Thus, it is possible that

Vezatin is expressed in the central nervous system, and enriched in dendrites of hippocampal neurons. Vezatin colocalizes with PSD95, indicating that vezatin is a postsynaptic protein at excitatory synapses (Danglot et al., 2012). In cultured, vezt-deficient hippocampal neurons, dendritic branching is reduced (Sanda et al., 2010). Moreover, in mice that are deficient in neuronal vezatin, dendritic spines of hippocampal neurons appear stubby, indicating a role for vezatin in regulating spine formation and maturation (Danglot et al., 2012). Because these deficits resemble the morphological abnormalities at the neuromuscular synapse of vezt mutant mice, vezatin may have a conserved role in shaping the postsynaptic membrane in the peripheral and central nervous systems.

MATERIALS AND METHODS
Animals
Mice were housed and maintained according to Institutional Animal Care and Use Committee guidelines. Mice carrying floxed and null alleles of vezt and null alleles of rapsn have been described previously (Gautam et al., 1995; Hyenne et al., 2007). vezt mutant mice were graciously provided by Christianne Petit (Institut Pasteur) and Marie-Christine Simmler (Université Paris, Institut Jacques Monod). Mice carrying a hsa::cre transgene, which confers Cre recombinase expression in myofibers, has been described previously (Miniou et al., 1999).

Mass spectrometry
Following enrichment using α-BGT affinity isolation, proteins were separated by SDS–PAGE, digested with trypsin, and analyzed by LC-MS/MS (Thermo Scientific LTQ Orbitrap MS coupled directly to a Waters NanoAquity UPLC). Peptides were separated on a self-packed 75 mm ID × 15 cm C18 column with a 2–45% gradient of acetonitrile in 0.1% formic acid. The LTQ Orbitrap was operated in data-dependent MSMS mode with MS (Orbitrap) resolution of 60,000. MS/MS scan information was extracted by DTASuper-Charge to generate Mascot generic files (.mgf), which were used to search a forward and reverse mouse/rat National Center for Biotechnology Information database using Mascot v2.1. Raw data files and Mascot search results were used to identify and quantify proteins by MSQuant v1.16. MSQuant results for changing proteins were verified manually, and redundant protein identifications were clustered using ProteinCenter v1.2.2 (Proxeon) at the 95% homology level. Protein-weighted average abundances (weighted based on the number of peptides/protein) were normalized to the weighted abundances of the AChR subunits. Of the 278 proteins that were identified and quantified, we identified six proteins that coisolated with AChRs and increased their association with AChRs following agrin stimulation, based on a 2 SD difference from mean ratios (ratios greater than 1.23 or less than 0.77).

Myoblasts grown in vitro
C2C12 cells (ATCC Cat# CRL-1772; RRID:CVCL_0188) were grown in growth medium (GM), which consisted of DMEM (4.5 g/l glucose, L-glutamine, and sodium pyruvate), supplemented with 10% fetal bovine serum (FBS), at 37° in 6.0% CO_2. Differentiation was induced at 80% confluency in DMEM (4.5 g/l glucose, L-glutamine without sodium pyruvate), supplemented with 2% heat inactivated horse serum.

Limbs from E17.5–E18.5 embryos were collected and separated from cartilage and bone in oxygenated L-15 media. Muscles were minced and digested in 5 mg/ml papain, reconstituted in Hanks' balanced salt solution (+$CaCl_2$ and $MgCl_2$), for 30 min at 37°C with mild shaking every 5 min. Digested tissue was serially triturated with small bore fire-polished pipettes in 20% FBS in DMEM/F12, passed through 40-μm cell strainers and plated on Matrigel (Corning)-coated tissue culture plates at a high density for rapid differentiation of myoblasts. Antibodies to myosin (1:2000; Sigma-Aldrich Cat# M4276; RRID:AB_477190) were used to stain differentiated myotubes. Myoblasts were differentiated into myotubes, and 3 d later, myotubes were treated with 500 pM agrin for 12 h (R&D, Minneapolis, MN). Cultures were labeled with Alexa 594–conjugated α-BGT (Invitrogen) for 1 h at 37°C, washed with DMEM, and subsequently maintained without agrin for 0–12 h.

Western blotting and AChR pull down
C2C12 myotubes or muscle from mice were used to generate muscle lysates. Whole leg muscles from E17.5–E18.5 or P60 mice were homogenized in MuSK lysis buffer (50 mM sodium chloride, 30 mM triethanolamine, pH 7.5, 50 mM sodium flouride, 5 mM EDTA, 5 mM ethylene glycol-bis(β-aminoethyl ether)-N,N,N',N'-tetraacetic acid [EGTA], 2 mM sodium orthovanadate, 1 mM N-ethylmaleimide, 1 mM sodium tetrathionate, 1 μg/ml pepstatin plus complete protease inhibitors; Roche, Basel, Switzerland) with a PT 10/35 Polytron (Kinematica AG, Littau-Lucerne, Switzerland) at 4°C. NP-40 was then added to a final concentration of 1%. We inhibited tyrosine kinases by preincubating C2 myotubes with 20 nM staurosporine or 1 μM herbimycin for 5 h, followed by agrin treatment in the presence of inhibitors. Myotubes were treated with 100 pM agrin (R&D, Minneapolis, MN) for 40 min at 37°C before collecting and lysing cells (30 min) or tissue (1 h) at 4°C in MuSK buffer (50 mM sodium chloride, 30 mM triethanolamine, pH 7.5, 50 mM sodium flouride, 5 mM EDTA, 5 mM EGTA, 2 mM sodium orthovanadate, 1 mM N-ethylmaleimide, 1 mM sodium tetrathionate, 1 μg/ml pepstatin plus complete protease inhibitors; Roche, Basel, Switzerland). Lysates were cleared of insoluble debris by centrifugation of 20 min at 14,000 rpm at 4°C and then precleared with streptavidin agarose beads (ThermoFisher Scientific) for 1 h at 4°C. Protein levels in lysates were determined using standard Bradford assays, and a constant amount of protein was incubated with 10^{-8} M biotin–α-BGT (Invitrogen, Carlsbad, CA) for 1 h at 4°C and then incubated with streptavidin agarose beads for 4 h or overnight at 4°C. Proteins were eluted in 2X SDS–PAGE buffer by heating at 65°C for 10 min, resolved by SDS–PAGE (6% or 8% acrylamide; Invitrogen) and transferred to polyvinylidene fluoride membranes. Western blots were probed with antibodies to the AChR β-subunit (Sigma-Aldrich; Cat# N8283; RRID:AB_262151), rapsyn (Abcam; Cat# ab156002; RRID:AB_298028), α-actinin (ThermoFisher Scientific; Cat# A304-768A; RRID:AB_2620963), annexin A2 (Abcam; Cat# ab41803; RRID:AB_940267), enolase 1 (Cell Signaling Technology; Cat# 3810; RRID:AB_2246524), and β-actin 1:5000, Sigma-Aldrich Cat# A2228, RRID:AB_476697). We quantified the band intensities with a Chemi-Doc imaging system (BioRad), as described previously (Remedio et al., 2016). The band intensity for each protein was normalized to the band intensity of the AChR β subunit, and the graphs show the mean values from three separate experiments. The Wilcoxon-Mann-Whitney test was used to determine statistical significance and was conducted using GraphPad Prism 6.0 software.

CD4-AChR subunit chimera expression, extraction, and immunoprecipitation
CD4-AChR subunit chimeras were a kind gift from Michael Ferns (University of California, Davis). HEK 293T cells were transfected with cDNAs encoding CD4-AChR subunit chimeras and either Flag-vezatin or both Flag-vezatin and rapsyn-HA using lipofectamine 3000 following the manufacturer's instructions (ThermoFisher

Scientific). Forty-eight hours posttransfection, cells were collected and resuspended in extraction buffer (0.5% Triton X-100, 25 mM Tris, 25 mM glycine, 150 mM NaCl, 5 mM EDTA, and the protease inhibitors PMSF, benzamidine, N-ethylmaleimide, and $Na_2S_4O_6$) and incubated for 10 min on ice. Insoluble proteins were removed by centrifugation at 13,000 rpm for 5 min. The CD4 chimeras were immunoprecipitated from the soluble fraction with monoclonal antibody GK1.5 (BD Biosciences-Pharmingen) bound to Protein G-Dynabeads (ThermoFisher Scientific) for 1 h at RT. The beads were washed four times with lysis buffer, and resuspended in 2X SDS protein loading buffer (SDS, glycerol, 10% β-mercaptoethanol, and bromophenol blue) and heated at 65°C for 10 min before SDS–PAGE. The solubilized proteins were separated in 10% polyacrylamide gels, and the blots were probed with antibodies to CD4 (1:2000; Abcam; Cat# ab183685; RRID:AB_2686917), Flag (1:2000; Sigma-Aldrich; Cat# F1804; RRID:AB_262044), or HA (1:2000; Sigma-Aldrich Cat# H9658; RRID:AB_260092).

Whole mount diaphragm muscle staining
Diaphragm muscles were dissected from E17.5–18.5, P60 or P180 mice in oxygenated L-15 media, fixed for 1.5 h in 1% paraformaldehyde (PFA), blocked for 1 h in 3% bovine serum albumin (BSA)/0.5% Triton X-100/ phosphate-buffered saline (PBS). Primary antibodies were diluted in 3% BSA/0.5% Triton X-100/PBS and forced pipetted into tissue, which was incubated overnight in a humidified chamber at 4°C with gentle agitation. Antibodies to neurofilament-L (1:3000, Synaptic systems; Cat# 171002; RRID:AB_887743), Synapsin 1/2 (1:2000; Synaptic systems; embryonic Cat# 106002 RRID:AB_887804), or β-tubulin (1:3000, Synaptic systems; Cat# 302302, RRID:AB_10637424) were used to label motor axons and nerve terminals. After extensive washing (5 h in 0.5% Triton X-100/PBS at room temperature), whole mounts of diaphragm muscles were incubated with secondary antibodies and Alexa 594–conjugated α-BGT (Invitrogen; in PBS with 3% BSA/0.5% Triton X-100) in a humidified chamber overnight at 4°C with gentle agitation. Diaphragm muscles were washed extensively and rinsed in PBS before mounting in Vectashield (Vector Laboratories). Images were acquired with a Zeiss LSM 700 or 800 confocal microscope, and the number and size of AChR clusters and the density of synaptic AChRs were determined using Volocity 3D imaging software (Perkin Elmer), as described previously (Jaworski and Burden, 2006). Low-magnification images were captured on a Zeiss Axio Zoom V16 fluorescence stereomicroscope. The distributions of AChRs and nerve terminals were determined by measuring the pixel value in 100-µm strips of the diaphragm muscle using Fiji software, as described previously (Kim and Burden, 2008).

Electron microscopy
Electron microscopy was performed as described previously (Friese et al., 2007). Briefly, diaphragm muscles were dissected in oxygen-saturated L15 at 37°C. Muscles were treated with 1 µg/ml TTX (tetrodotoxin) for 10 min. Following TTX treatment, muscles were fixed with glutaraldehyde for 1 h, while forcing fixative into the tissue. Muscles were then treated with 0.1M Tris buffer for 30 min on a shaker, washed with iso-osmotic phosphate buffer for 30 min, treated with 1% osmium for 1–2 h in a fume hood and washed with water for 1 h on a shaker. Samples were treated with saturated uranyl acetate in water for 1 h, washed with water for 1–2 h and dehydrated with ethanol. Muscles were freed from ribs with a razor blade, transferred into glass scintillation vials containing propylene oxide, and washed twice for 30 min. Samples were infiltrated with propylene oxide:epon (1:1) for 1 h, with slow rocking, followed by epon (without accelerator) overnight, and embedded in epon with accelerator at 60°C overnight.

Cryosection immunostaining
Hindlimb muscles from P30 mice were fixed in 1% PFA in PBS for 1 h at 4°C, rinsed twice at 4°C in PBS, cryoprotected (in 30% sucrose-PBS) overnight at 4°C, and embedded in TissueTek (Sakura, Tokyo, Japan). Frozen sections (10 µm) were stained with the following antibodies: MuSK (1:1000; #83033; Herbst et al., 2002), rapsyn (1:1000, ThermoFisher Scientific; Cat# MA1-746; RRID:AB_2177611), synapsin (1:2000, Synaptic Systems; Cat# 106002 RRID:AB_887804), and vezatin (1:1000; gift from Christine Petite). Images were acquired with a 40× (1.4 NA) objective on a Zeiss LSM 700 confocal microscope.

Single fiber dissociation and staining
Hindlimbs were fixed in 2% PFA for 2 h at room temperature. Samples were rinsed twice, and individual muscles were dissected and fixed with 2% PFA for an additional 1 h at room temperature for an additional hour. Muscle fibers were teased and plated on poly-L-lysine–coated coverslips. For immunostaining, muscle fibers were blocked at room temperature for 2 h at room temperature in 0.04% saponin and 1% BSA and then incubated overnight with primary antibodies. The following day, muscles were rinsed in blocking buffer for 1 h at room temperature and incubated with secondary antibodies for 2 h at room temperature. Samples were washed for 1 h at room temperature and mounted in Vetashield (Vector Laboratories).

Behavior
Forelimb and all-limb muscle strength of P60 male mice were determined using a grip force tensiometer (Bioseb). Mice were held by their tails and allowed to grip a grid that was connected to the grip strength meter; the mice were gently pulled horizontally until their grip was released. Five trials were conducted; forelimb and all limb tests were separated by a 20- to 30-min interval. Force (g) was averaged from the three maximum scores and this value was normalized to body weight (g). Motor function of P60 male mice was assessed on a RotaRod (AccuRotor four-channel; Omnitech Electronics). Mice were placed on the RotaRod (3.0-cm rotating cylinder) rotating at 2.5 rpm, and the speed of rotation was increased linearly to 40 rpm over the course of 5 min. The time to fall from the rod was determined. Each mouse was subjected to three trials with 5-min intervals, and the longest latency to fall from the three trials was recorded. Motor fatigue was assessed in P60 male mice using an inverted wire hang test. Individual mice were placed on a wire that was supported by two columns 27 cm apart, mounted 60 cm above a padded laboratory bench. After gently placing the forelimbs on the wire, the time to fall from the wire was determined. The longest latency was recorded to fall from three trials, separated by 15–30 min.

REFERENCES

Antolik C, Catino DH, O'Neill AM, Resneck WG, Ursitti JA, Bloch RJ (2007). The actin binding domain of ACF7 binds directly to the tetratricopeptide repeat domains of rapsyn. Neuroscience 145, 56–65.

Bahloul A, Simmler MC, Michel V, Leibovici M, Perfettini I, Roux I, Weil D, Nouaille S, Zuo J, Zadro C, et al. (2009). Vezatin, an integral membrane protein of adherens junctions, is required for the sound resilience of cochlear hair cells. EMBO Mol Med 1, 125–138.

Banks GB, Fuhrer C, Adams ME, Froehner SC (2003). The postsynaptic submembrane machinery at the neuromuscular junction: requirement for rapsyn and the utrophin/dystrophin-associated complex. J Neurocytol 32, 709–726.

Borges LS, Yechikhov S, Lee YI, Rudell JB, Friese MB, Burden SJ, Ferns MJ (2008). Identification of a motif in the acetylcholine receptor β subunit whose phosphorylation regulates rapsyn association and postsynaptic receptor localization. J Neurosci 28, 11468–11476.

Burden S (1977). Development of the neuromuscular junction in the chick embryo: the number, distribution, and stability of acetylcholine receptors. Dev Biol 57, 317–329.

Burden SJ (1993). Synapse-specific gene expression. Trends Genet 9, 12–16.

Burden SJ (1998). The formation of neuromuscular synapses. Genes Dev 12, 133–148.

Burden SJ, DePalma RL, Gottesman GS (1983). Crosslinking of proteins in acetylcholine receptor-rich membranes: association between the β-subunit and the 43 kd subsynaptic protein. Cell 35, 687–692.

Burden SJ, Huijbers MG, Remedio L (2018). Fundamental molecules and mechanisms for forming and maintaining neuromuscular synapses. Int J Mol Sci, doi: 10.3390/ijms19020490.

Burden SJ, Yumoto N, Zhang W (2013). The role of MuSK in synapse formation and neuromuscular disease. Cold Spring Harb Perspect Biol 5, a009167.

Chen F, Qian L, Yang ZH, Huang Y, Ngo ST, Ruan NJ, Wang J, Schneider C, Noakes PG, Ding YQ, et al. (2007). Rapsyn interaction with calpain stabilizes AChR clusters at the neuromuscular junction. Neuron 55, 247–260.

Cifuentes-Diaz C, Goudou D, Mege RM, Velasco E, Nicolet M, Herrenknecht K, Rubin L, Rieger F (1998). Distinct location and prevalence of α-, β-catenins and γ-catenin/plakoglobin in developing and denervated skeletal muscle. Cell Adhes Commun 5, 161–176.

Cifuentes-Diaz C, Goudou D, Padilla F, Facchinetti P, Nicolet M, Mege RM, Rieger F (1996). M-cadherin distribution in the mouse adult neuromuscular system suggests a role in muscle innervation. Eur J Neurosci 8, 1666–1676.

Cifuentes-Diaz C, Nicolet M, Goudou D, Rieger F, Mege RM (1994). N-cadherin expression in developing, adult and denervated chicken neuromuscular system: accumulations at both the neuromuscular junction and the node of Ranvier. Development 120, 1–11.

Couteaux R (1955). Localization of cholinesterases at neuromuscular junctions. Int Rev Cytol IV, 335–371.

Danglot L, Freret T, Le Roux N, Narboux Neme N, Burgo A, Hyenne V, Roumier A, Contremoulins V, Dauphin F, Bizot JC, et al. (2012). Vezatin is essential for dendritic spine morphogenesis and functional synaptic maturation. J Neurosci 32, 9007–9022.

Dobbins GC, Luo S, Yang Z, Xiong WC, Mei L (2008). α-Actinin interacts with rapsyn in agrin-stimulated AChR clustering. Mol Brain 1, 18.

Donaldson JG (2003). Multiple roles for Arf6: sorting, structuring, and signaling at the plasma membrane. J Biol Chem 278, 41573–41576.

Donaldson JG, Porat-Shliom N, Cohen LA (2009). Clathrin-independent endocytosis: a unique platform for cell signaling and PM remodeling. Cell Signal 21, 1–6.

Engel AG, Shen XM, Selcen D, Sine SM (2015). Congenital myasthenic syndromes: pathogenesis, diagnosis, and treatment. Lancet Neurol 14, 420–434.

Fertuck HC, Salpeter MM (1976). Quantitation of junctional and extrajunctional acetylcholine receptors by electron microscope autoradiography after 125I-α-bungarotoxin binding at mouse neuromuscular junctions. J Cell Biol 69, 144–158.

Friese MB, Blagden CS, Burden SJ (2007). Synaptic differentiation is defective in mice lacking acetylcholine receptor β-subunit tyrosine phosphorylation. Development 134, 4167–4176.

Froehner SC, Gulbrandsen V, Hyman C, Jeng AY, Neubig RR, Cohen JB (1981). Immunofluorescence localization at the mammalian neuromuscular junction of the Mr 43,000 protein of Torpedo postsynaptic membranes. Proc Natl Acad Sci USA 78, 5230–5234.

Fuhrer C, Hall ZW (1996). Functional interaction of Src family kinases with the acetylcholine receptor in C2 myotubes. J Biol Chem 271, 32474–32481.

Gautam M, Noakes PG, Moscoso L, Rupp F, Scheller RH, Merlie JP, Sanes JR (1996). Defective neuromuscular synaptogenesis in agrin-deficient mutant mice. Cell 85, 525–535.

Gautam M, Noakes PG, Mudd J, Nichol M, Chu GC, Sanes JR, Merlie JP (1995). Failure of postsynaptic specialization to develop at neuromuscular junctions of rapsyn-deficient mice. Nature 377, 232–236.

Grady RM, Akaaboune M, Cohen AL, Maimone MM, Lichtman JW, Sanes JR (2003). Tyrosine-phosphorylated and nonphosphorylated isoforms of alpha-dystrobrevin: roles in skeletal muscle and its neuromuscular and myotendinous junctions. J Cell Biol 160, 741–752.

Grady RM, Merlie JP, Sanes JR (1997). Subtle neuromuscular defects in utrophin-deficient mice. J Cell Biol 136, 871–882.

Grady RM, Zhou H, Cunningham JM, Henry MD, Campbell KP, Sanes JR (2000). Maturation and maintenance of the neuromuscular synapse: genetic evidence for roles of the dystrophin–glycoprotein complex. Neuron 25, 279–293.

Hall ZW, Sanes JR (1993). Synaptic structure and development: the neuromuscular junction. Cell 72 (suppl), 99–121.

Herbst R, Avetisova E, Burden SJ (2002). Restoration of synapse formation in Musk mutant mice expressing a Musk/Trk chimeric receptor. Development 129, 5449–5460.

Hyenne V, Louvet-Vallee S, El-Amraoui A, Petit C, Maro B, Simmler MC (2005). Vezatin, a protein associated to adherens junctions, is required for mouse blastocyst morphogenesis. Dev Biol 287, 180–191.

Hyenne V, Souilhol C, Cohen-Tannoudji M, Cereghini S, Petit C, Langa F, Maro B, Simmler MC (2007). Conditional knock-out reveals that zygotic vezatin-null mouse embryos die at implantation. Mech Dev 124, 449–462.

Jaworski A, Burden SJ (2006). Neuromuscular synapse formation in mice lacking motor neuron- and skeletal muscle-derived Neuregulin-1. J Neurosci 26, 655–661.

Kim N, Burden SJ (2008). MuSK controls where motor axons grow and form synapses. Nat Neurosci 11, 19–27.

Kim N, Stiegler AL, Cameron TO, Hallock PT, Gomez AM, Huang JH, Hubbard SR, Dustin ML, Burden SJ (2008). Lrp4 is a receptor for Agrin and forms a complex with MuSK. Cell 135, 334–342.

Kummer TT, Misgeld T, Lichtman JW, Sanes JR (2004). Nerve-independent formation of a topologically complex postsynaptic apparatus. J Cell Biol 164, 1077–1087.

Kussel-Andermann P, A. El-Amraoui, Safieddine S, Nouaille S, Perfettini I, Lecuit M, Cossart P, Wolfrum U, Petit C (2000). Vezatin, a novel transmembrane protein, bridges myosin VIIA to the cadherin-catenins complex. EMBO J 19, 6020–6029.

Latvanlehto A, Fox MA, Sormunen R, Tu H, Oikarainen T, Koski A, Naumenko N, Shakirzyanova A, Kallio M, Ilves M, et al. (2010). Muscle-derived collagen XIII regulates maturation of the skeletal neuromuscular junction. J Neurosci 30, 12230–12241.

Lee Y, Rudell J, Ferns M (2009). Rapsyn interacts with the muscle acetylcholine receptor via α-helical domains in the α, β, and ε subunit intracellular loops. Neuroscience 163, 222–232.

Li L, Cao Y, Wu H, Ye X, Zhu Z, Xing G, Shen C, Barik A, Zhang B, Xie X, et al. (2016). Enzymatic activity of the scaffold protein Rapsyn for synapse formation. Neuron 92, 1007–1019.

Lin W, Burgess RW, Dominguez B, Pfaff SL, Sanes JR, Lee KF (2001). Distinct roles of nerve and muscle in postsynaptic differentiation of the neuromuscular synapse. Nature 410, 1057–1064.

Luiskandl S, Woller B, Schlauf M, Schmid JA, Herbst R (2013). Endosomal trafficking of the receptor tyrosine kinase MuSK proceeds via clathrin-dependent pathways, Arf6 and actin. FEBS J 280, 3281–3297.

Martinez-Pena y Valenzuela I, Mouslim C, Akaaboune M (2010). Calcium/calmodulin kinase II-dependent acetylcholine receptor cycling at the mammalian neuromuscular junction in vivo. J Neurosci 30, 12455–12465.

McMahan UJ (1990). The agrin hypothesis. Cold Spring Harb Symp Quant Biol 55, 407–418.

Miniou P, Tiziano D, Frugier T, Roblot N, Le Meur M, Melki J (1999). Gene targeting restricted to mouse striated muscle lineage. Nucleic Acids Res 27, e27.

Muller JS, Mihaylova V, Abicht A, Lochmuller H (2007). Congenital myasthenic syndromes: spotlight on genetic defects of neuromuscular transmission. Expert Rev Mol Med 9, 1–20.

Neubig RR, Krodel EK, Boyd ND, Cohen JB (1979). Acetylcholine and local anesthetic binding to Torpedo nicotinic postsynaptic membranes after removal of nonreceptor peptides. Proc Natl Acad Sci USA 76, 690–694.

Oury J, Liu Y, Topf A, Todorovic S, Hoedt E, Preethish-Kumar V, Neubert TA, Lin W, Lochmuller H, Burden SJ (2019). MACF1 links Rapsyn to microtubule- and actin-binding proteins to maintain neuromuscular synapses. J Cell Biol 218, 1686–1705.

Remedio L, Gribble KD, Lee JK, Kim N, Hallock PT, Delestree N, Mentis GZ, Froemke RC, Granato M, Burden SJ (2016). Diverging roles for Lrp4 and Wnt signaling in neuromuscular synapse development during evolution. Genes Dev 30, 1058–1069.

Sanda M, Ohara N, Kamata A, Hara Y, Tamaki H, Sukegawa J, Yanagisawa T, Fukunaga K, Kondo H, Sakagami H (2010). Vezatin, a potential target for ADP-ribosylation factor 6, regulates the dendritic formation of hippocampal neurons. Neurosci Res 67, 126–136.

Sanes JR, Lichtman JW (2001). Induction, assembly, maturation and maintenance of a postsynaptic apparatus. Nat Rev Neurosci 2, 791–805.

Schaeffer L, de Kerchove d'Exaerde A, Changeux JP (2001). Targeting transcription to the neuromuscular synapse. Neuron 31, 15–22.

Serdaroglu P, Askanas V, Engel WK (1992). Immunocytochemical localization of ubiquitin at human neuromuscular junctions. Neuropathol Appl Neurobiol 18, 232–236.

Shi L, Fu AK, Ip NY (2012). Molecular mechanisms underlying maturation and maintenance of the vertebrate neuromuscular junction. Trends Neurosci 35, 441–453.

Slater CR (2017). The structure of human neuromuscular junctions: some unanswered molecular questions. Int J Mol Sci 18, doi: 10.3390/ijms18102183.

Smith CL, Mittaud P, Prescott ED, Fuhrer C, Burden SJ (2001). Src, Fyn, and Yes are not required for neuromuscular synapse formation but are necessary for stabilization of agrin-induced clusters of acetylcholine receptors. J Neurosci 21, 3151–3160.

Sobel A, Heidmann T, Hofler J, Changeux JP (1978). Distinct protein components from Torpedo marmorata membranes carry the acetylcholine receptor site and the binding site for local anesthetics and histrionicotoxin. Proc Natl Acad Sci USA 75, 510–514.

Sousa S, Cabanes D, El-Amraoui A, Petit C, Lecuit M, Cossart P (2004). Unconventional myosin VIIa and vezatin, two proteins crucial for *Listeria* entry into epithelial cells. J Cell Sci 117, 2121–2130.

Tintignac LA, Brenner HR, Ruegg MA (2015). Mechanisms regulating neuromuscular junction development and function and causes of muscle wasting. Physiol Rev 95, 809–852.

Valdez G, Tapia JC, Kang H, Clemenson GD Jr, Gage FH, Lichtman JW, Sanes JR (2010). Attenuation of age-related changes in mouse neuromuscular synapses by caloric restriction and exercise. Proc Natl Acad Sci USA 107, 14863–14868.

Wang J, Jing Z, Zhang L, Zhou G, Braun J, Yao Y, Wang ZZ (2003). Regulation of acetylcholine receptor clustering by the tumor suppressor APC. Nat Neurosci 6, 1017–1018.

Weatherbee SD, Anderson KV, Niswander LA (2006). LDL-receptor-related protein 4 is crucial for formation of the neuromuscular junction. Development 133, 4993–5000.

Wood SJ, Slater CR (2001). Safety factor at the neuromuscular junction. Prog Neurobiol 64, 393–429.

Wu H, Xiong WC, Mei L (2010). To build a synapse: signaling pathways in neuromuscular junction assembly. Development 137, 1017–1033.

Yamanashi Y, Tezuka T, Yokoyama K (2012). Activation of receptor protein-tyrosine kinases from the cytoplasmic compartment. J Biochem 151, 353–359.

Yang X, Arber S, William C, Li L, Tanabe Y, Jessell TM, Birchmeier C, Burden SJ (2001). Patterning of muscle acetylcholine receptor gene expression in the absence of motor innervation. Neuron 30, 399–410.

Zhang B, Luo S, Dong XP, Zhang X, Liu C, Luo Z, Xiong WC, Mei L (2007). β-Catenin regulates acetylcholine receptor clustering in muscle cells through interaction with rapsyn. J Neurosci 27, 3968–3973.

Zhang B, Luo S, Wang Q, Suzuki T, Xiong WC, Mei L (2008). LRP4 serves as a coreceptor of agrin. Neuron 60, 285–297.

Zuber B, Unwin N (2013). Structure and superorganization of acetylcholine receptor-rapsyn complexes. Proc Natl Acad Sci USA 110, 10622–10627.